α,ε-Hybrid Foldamers with 1,2,3-Triazole Rings: Order versus Disorder

α,ε-Hybrid Foldamers with 1,2,3-Triazole Rings: Order versus Disorder

Lorenzo Milli,† Michele Larocca,† Mattia Tedesco,‡ Nicola Castellucci,† Elena Ghibaudi,‡ Andrea Cornia,§
Matteo Calvaresi,† Francesco Zerbetto,† and Claudia Tomasini*,†

†Dipartimento di Chimica "G. Ciamician", Alma Mater Studiorum Universita di Bologna, Via F. Selmi 2, 40126 Bologna, Italy

‡Dipartimento di Chimica, Universita di Torino, Via P. Giuria 7, 10125 Torino, Italy

§Department of Chemical and Geological Sciences, University of Modena and Reggio Emilia & INSTM Research Unit, Via G. Campi 183, 41125 Modena, Italy

ABSTRACT: Two epimeric series of foldamers characterized by the presence of a repeating α,ε-dipeptide unit have been prepared and characterized by 1H NMR and ECD spectroscopies together with X-ray diffraction. The first series contains L-Ala and D-4-carboxy-5-methyl-oxazolidin-2-one (D-Oxd). The other series contains L-Ala and L-Oxd. The L,D series of oligomers forms ordered β-turn foldamers, characterized by a 311 pattern. The L,L series is not ordered. Simulations show that an ordered L,L trimer lies more than 2 kcal/mol higher than the more stable nonfolded extended conformations. Cu2+ forms complexes with both series but is not able to order the L,L series. Analysis of the EPR spectra shows that the L,D foldamers bear two types of complexation sites that are assigned as a nitrogen donor of the triazole ring and a carboxylate ligand. The L-Ala-D-Oxd-Tri-CO motif may be introduced in any peptide sequence requiring the presence of a stable β-turn conformations, like in the study of protein−protein interactions.

INTRODUCTION

Pseudopeptide foldamers are synthetic molecules able to organize in well-defined secondary structures (i.e., helices,
turns, and sheets). Despite their small size, they truly mimic biomacromolecules.1 Their repetitive secondary structure is
imparted by conformational restrictions of the monomeric unit.2 Since 1996, when the neologism was coined, this research field has blossomed; many groups have explored oligomers with a wide backbone variety as potential foldamers, and several reviews have been published.3 In the past few years, we have extensively studied the conformational behavior of foldamers that contain the 4-carboxy-5-methyloxazolidin-2-one (Oxd) moiety.4 Acylation of the Oxd units yields imides that behave like rigid spacers, and the relative conformation of the two carbonyls generates a trans conformation with respect to the adjacent peptide bond.5 Among them, we have also investigated hybrid foldamers, where the Oxd moiety is alternated with an α- or a β-amino acid. In this case, the relative configuration of the Oxd and of the alternating amino acid are of paramount importance. For instance, the L-Ala-D-Oxd series tends to form β-bend ribbon spirals, while the L-Ala-L-Oxd series does not.6 Important stimulation came from the suggestion to employ dipeptide repeat units of various homologous amino acids.7 α/β-Hybrid peptides containing α- and β-amino acid constituents in a 1:1 backbone alternation displayed a variety of helical structures.8 Some of these peptides elicited substantial biological activity.9 The concept was successfully extended to α/γ-, α/δ-, and β/γ-hybrid peptides.10 Recently, we have developed the synthesis of new preorganized dipeptide units that contain a 1,2,3-triazole (Tri) ring close to the Oxd group (Figure 1) and that mimic a constrained α,β-dipeptide moiety.11 The presence of the two heterocycles imparts a rigid trans conformation to the chain. The two rings differ for their spatial arrangement in that Oxd is chiral and 3,4-disubstituted while Tri is flat, achiral, and 1,4-disubstituted. The nitrogen

of the Tri moiety cannot form a hydrogen bond, and the α,β-dipeptide moiety may be considered as a single unit, which constitutes a constrained mimic of ε-amino acid.12

2. Conformational Analysis. Preliminary information on the preferred conformation of the oligomers of both series was obtained by 1H NMR and ECD absorption spectra in solution. These outcomes were further analyzed by single-crystal X-ray diffraction and molecular dynamics calculations. FT-IR spectroscopy in CH2Cl2 solution gave no useful information since we could not find any evidence for the formation of intramolecular N−H···O=C hydrogen bonds,21 as no stretching bands below 3400 cm−1 were detected.

2.1. 1H NMR spectroscopy. By 1H NMR spectroscopy we confirmed the identity of all compounds. ROESY experiments performed on Boc-(L-Ala-D-Oxd-Tri-CO)3-OBn 9 and Boc-(LAla-L-Oxd-Tri-CO)3-OBn 15 gave information on the preferred conformation of the two oligomers. All experiments were recorded with a mixing time of 0.400 s for both samples (Figure 3). Besides the trivial couplings, the ROESY spectrum of 9 in CDCl3 shows cross peaks that have been attributed to the interaction of the triazole C−H with the amide NH and with the alanine CH (see the Supporting Information). The outcome suggests the formation of a preferred bent conformation. Unfortunately, 15 was poorly soluble in CDCl3, which forced us to record the ROESY spectrum in CD3OD. The fast exchange between the NH of the amide moieties and the deuterated solvent prevented the analysis of cross peaks that involve the amide NH, and we could record only the cross peaks between the triazole C−H and the alanine Me groups.

2.2. ECD Spectroscopy. To avoid the strong signal due to the benzyl groups, ECD spectroscopy was perfomed on the
acids of both series, namely 6, 8, 10, 12, 14, and 16. In Figure 4 the per-residue ECD spectra of the oligomers of both series are reported. The spectra were recorded for 5 mM solutions in an 8:2 methanol/water mixture. The analysis of the preferred conformation of these compounds is not straightforward. These oligomers contain unusual structures that cannot easily be compared with α-amino acid oligomers. Nevertheless some information can be obtained from the comparison of these ECD spectra: the spectra of the L,L series shown in Figure 4b are very similar and display a strong negative band at 200−204 nm and a broad positive featureless band between 220 and 260 nm. These ECD spectra are strongly reminiscent of random coils. By contrast, the ECD spectra of the L,D series (Figure 4a) differ from each other and suggest the appearance of a secondary structure in dimer 8 and trimer 10. Comparison with previous data,22 as well as the analogy between triazole and proline rings, suggests the assignment of the ~200 nm band to a β-turn that may form by hydrogen bonding between the oxygen of the carbamate group (Boc) and the proton on the 1,2,3-triazole at position 5. The CD spectra of compounds 8 and 10 display two positive bands of comparable intensity at ~210 and ~228 nm, which recall an atypical helical structure.In fact, apart from the sign of the Cotton effect, these features are typical of right-handed helix-310 structures.23 On the other hand, the ratio between the intensities of the two bands does
not fully correspond to such structures. Taking into account the presence of a rigid triazole ring within the structure, by analogy with previous data, an atypical helix structure may be hypothesized, assuming that triazole is responsible for the inversion of the Cotton effect. Based on the experimental evidence, we propose that the monomer, dimer, and trimer of the L,D series, i.e., compounds 6, 8, and 10, exhibit a β-turn responsible for the absorption at low wavelength. Chain elongation allows further structuring, stabilized by intramolecular hydrogen bonds.

2.3. Single-Crystal X-ray Diffraction. Crystals of 5 and 7· 0.5C6H6 suitable for X-ray diffraction were grown as long needles by slowly evaporating solutions of 5 and 7 in benzene and benzene/methyl tert-butyl ether 1:1 v/v, respectively. Crystal data and refinement parameters for the two structures can be found in Table S1 (Supporting Information). In compound 5, the peptide folding mimics the β-turn structure of proteinogenic α-amino acids (Figure 5). The carbon atom C10 of the triazole is engaged in a nonclassical hydrogen interaction with the carboxyl oxygen O6 of the Boc group [d(H10···O6) =2.14(2) Å], resulting in an 11-membered hydrogen-bonded turn (311-helical structure). By consequence, the two fivemembered rings in the D-Oxd-Tri residue are forced in a syn conformation around the C11−C12 linkage. At the same time, the tBu carbon atom C23 of the Boc terminus is found at 3.51 Å from the center of the phenyl ring C2−C7, suggesting a CH/π interaction. The α-carbon atom of the L-Ala residue (C17) has an intramolecular H-contact with the endocyclic carbonyl oxygen O4 of the D-Oxd fragment [d(H17···O4) = 2.17(2) Å]. A similar pattern of intramolecular H-interactions, though with 0.2-Å longer H···A distances, is present in the C(O)-Ala2- D-Oxd2-Tri2 residue of 7·0.5C6H6, which also exhibits a surn structure (Figure 6). Inspection of the backbone torsion angles for the two compounds (Table 1) indeed reveals a remarkable similarity between the conformation of L-Ala-DOxd- Tri in monomer 5 and of L-Ala2-D-Oxd2-Tri2 in dimer 7; differences do not exceed 5° with the exception of the ϕ angle for the L-Ala and L-Ala2 residues. The above-mentioned α- carbon/C=O contact is repeated also within the L-Ala1-DOxd1 unit (H28···O8), which however, does not adopt a turn structure. In fact, the two five-membered rings are rotated away from each other around the C22−C23 bond, as shown by the large N8−C22−C23−N9 torsion angle (172.6(3)). Moreover, D-Oxd1-Tri1 and D-Oxd2-Tri2 entail opposite rotations of the triazole moiety around the CH2−N bond (N−N−C-C = −101.0(3)° vs 89.1(3)°). In the two compounds, the torsion angles are presented in Table 1. Overall, the torsion angles at the L-Ala residues (ϕ from −70.1 to −57.2° and ψ from 136.3 to 147.5°) are close to those typical for a PPII helix (ϕ = −79° and ψ = 150°). Turning now to crystal packing, the carbonyl C16−O5 and the amide N5-HN5 groups in 5 are involved in intermolecular hydrogen bonds directed approximately parallel to the b-axis [d(HN5···O5I) = 2.15(2) Å; I = x − 1/2, −y + 1/2, −z + 2]. These two H-bonds per molecule link the peptides into supramolecular zigzag chains running along the a-axis. In the crystal lattice, molecules of 7 are linked by a H-bond between the amide (N5) and triazole (N1) nitrogen atoms, with d(HN5···N1I) = 2.138(17) Å (I = x, y + 1, z). The second amide nitrogen N10 is also engaged in a H-bond with triazole nitrogen atom N7 of a neighboring molecule, but with a significantly longer distance [d(HN10···N7II) = 2.334(19) Å; II= −x, y − 1/2, −z]. Both intermolecular contacts are directed approximately parallel to the b-axis of the unit cell. It is noteworthy that the only NH···CO hydrogen bonds found in these structures are of the intermolecular type and occur in 5, in agreement with the results of FT-IR spectroscopy in solution. Detailed geometrical parameters for hydrogen interactions are gathered in Tables S2 and S3 (Supporting Information).

2.4. Molecular Dynamics. The inability to grow crystals of the trimers 9, 10, 15, or 16 suggested the use of alternative approaches to gain insight in their structures. Molecular dynamics simulations for 1 μs of the trimers Boc-(L-Ala-DOxd- Tri-CO)3-OBn 9 and Boc-(L-Ala-L-Oxd-Tri-CO)3-OBn 15 were carried out in an explicit methanol box, reproducing the conditions in which NMR spectra are registered. Principal component analysis (PCA) of the MD trajectories generated the free-energy landscapes of the two peptides (see the Experimental Section). This approach proved effective in reproducing the NMR and crystallographic data and provides insight into the free

energy landscape.25 The energy landscape of 9 is characterized by well-separated minima corresponding to specific conformational structures (Figure 7, see video V1 in the Supporting Information). The most populated conformer, Conf A, has a well-defined hydrogen-bond pattern that folds the peptide in a structurally stable turn structure. This 11-membered hydrogen-bonded turn corresponds to the motif identified in the solid state by the crystallographic analysis of the monomer 5 and dimer 7 (Table S4, Supporting Information). The other stable minima Conf B, Conf C, and Conf D maintain this structural motif, even if the other regions of the peptide show considerable conformational freedom (Figure 8). This area of the peptide energy landscape, characterized by the presence of the turn, is around 2−7 kcal mol−1 more stable than any other conformation (extended, helix-like, twist-like, Figure S1, Supporting Information). The nonstandard C−H··· O=C hydrogen bonds, represented by dashed lines in Figure 8, govern the structural stability of this motif. On the contrary, in the energy landscape of 15 (Figure 8) the local minima are broad, and there is no significant basin of attraction indicative of a folded conformation. The most populated Conf A and Conf B (Figure 8) represent nonfolded extended conformations of the peptide that undergo practically free rotation in the solvent (video V2, Supporting Information). A turn structure can still be identified (Figure S2, Supporting Information). It is located the region of PCA1 that ranges between 37 and 40, and its energy is more than 2 kcal/mol higher than the more stable minima. The β-turn structure of 9 is replaced by a γ-turn structure in 15 with a 7-membered hydrogen bonded ring. This structure usually competes with its 10-membered analogue (here 11 because of the presence of a ε - amino acid) typical of a β-turn. Steric hindrance and/or chirality stabilize/destabilize the two competing ring-structures.

2.5. Complexation with Cu2+. Triazole rings tend to interact with Cu2+ ions and form complexes. The extra stabilization energy provided by the interaction with Cu2+ could in principle be used to impart an ordered structure to both series of oligomers.

2.5.1. UV−vis Spectroscopy. UV−vis complexometric titrations show that oligomers 6, 8, and 10 interact with copper, giving rise to complexes. Table 2 presents the average KD values for the L,D series. The saturation threshold (i.e., the metal concentration corresponding to system saturation) increases with elongation of the pseudopeptide chain, due to the increase of putative metal-binding sites. The absence of absorption bands in the λ ~600 nm region suggests that we are dealing with type-II copper centers.

2.5.2. ECD Spectroscopy. Complexometric titrations of compounds 6, 8, and 10, monitored by ECD spectroscopy (Figure 9), showed that in all cases Cu2+ addition affects the intensity of the absorption bands without changing the spectral pattern. This suggests that copper leaves the folding unchanged as compared to the free ligand. This is supported by the lack of meaningful changes upon addition of an EDTA excess. Analogous titrations with 12, 14, and 16 oligomers did not produce significant variations of the spectra (Figures S3−S5, Supporting Information). We conclude that Cu2+ is not able to induce extra folding in either series of oligomers.

2.5.3. EPR Spectroscopy. The interaction of Cu2+ with ligands 6, 8, and 10 in MeOH/H2O 8:2 (v/v) was further characterized by EPR spectroscopy, and the corresponding spin-Hamiltonian parameters are summarized in Table 3. In all cases, two distinct complexation modes were highlighted: these correspond to at least two distinct metal binding sites, called a and b in Table 3. The EPR parameters, with values of $A_{\parallel} > 100 \times 10^{-4} cm^{-1}$, and the absence of absorption bands in the visible region of the electronic spectra suggest that, in all cases, the metal center is a type-II

copper site. Center a shows lower A∥ values (106−109× 10−4 cm−1) as compared to center b (125−133 × 10−4 cm−1). On the basis of these spectral parameters, center a was assigned to a nitrogen-coordinated copper (i.e., copper interacting with the triazole ring). Due to the similarity of its EPR parameters with those of Cu(H2O)62+, center b was assigned to an oxygenated ligand (i.e., a carboxylate). g⊥ < g∥ is typical of a distorted tetragonal geometry, with the unpaired electron located in the dx2−y2 orbital. The tetragonal distortion is further supported by the following evidence:

• g∥/A∥ ratios >222 × 10−4 cm−1 for center a and >177 × 10−4 cm−1 for center b. Square planar complexes exhibit much lower values ((105−135) × 10−4 cm−1).26 This also indicates that center a is more distorted than center b.

• The absence of electronic absorption bands in the visible region as, for complexes with strong tetragonal distortion, these bands shift toward the IR.27 The lower degree of distortion of center b as compared to center a is consistent with its assignment to the carboxyterminal site, since it is reasonable to expect a less conformationally constrained complex as compared to the triazole. Finally, according to Sakaguchi et al.,26 g∥ values >2.30 are consistent with predominantly ionic interactions and corroborate the assignments of binding sites a and b to a triazole and a carboxylate, respectively. In all cases, the addition of a 10-fold molar excess of EDTA caused the formation of a pale blue solution. The EPR spectral pattern of the pale blue solutions was typical of Cu2+−EDTA complexes. This indicates the complete disruption of the Cu2+complexes by EDTA.

CONCLUSION

The purpose of this work was the optimized synthesis, conformational analysis, and application of two epimeric series of foldamers characterized by the presence of a repeating α, ε - dipeptide units. The ε -unit contains two heterocycles: a 1,2,3-triazole (Tri) and a 4-carboxy-5-methyloxazolidin-2-one (Oxd), while the α-unit is an alanine moiety. Both heterocycles imparts a rigid trans conformation to the chain, but the two rings differ for their spatial arrangement, as Oxd is chiral and 3,4-disubstituted while Tri is flat, achiral, and 1,4-disubstituted. Two series of oligomers have been prepared: Boc-(L-Ala-DOxd-Tri-CO)n-OBn (L,D series) and Boc-(L-Ala-L-Oxd-Tri-CO)n-OBn (L,L series). All compounds, including dimers and trimers, were prepared with good yields and have been characterized by 1H NMR and ECD spectroscopies together with X-ray diffraction (when feasible). Then both trimers were subjected to conformational analysis by atomistic molecular dynamics simulations. While the L,D series of oligomers form ordered β-turn foldamers, characterized by a 311 pattern, the L,L series is disordered. They alsoshowed that an ordered L,L trimer lies more than 2 kcal/mol higher than the more stable non folded extended conformations. Further information was obtained by tritration of both series with Cu2+, which forms complexes with both series, but it is not able to order the L,L series. Finally, analysis of the EPR spectra showed that the L,D foldamers bear two types of complexation sites that are assigned as the nitrogen of the triazole ring and a carboxylate ligand. In conclusion, these results demonstrate that a small modification of the skeleton (D-Oxd versus L-Oxd) produces a dramatic variation in the properties of these new foldamers. While the L,L series is basically unordered, even when complexation with Cu2+ takes place, the L,D-series forms in any case a β-turn conformation, characterized by a 311 pattern and stabilized by a nonconventional C−H···O=C hydrogen bond. This conformation is extremely stable, as it is present in all the oligomers of this series. Molecular dynamic calculations show that it is more stable of about 2−7 kcal/mol than any other. These new foldamers containing the L-Ala-D-Oxd-Tri-CO motif may be introduced in any peptide sequence

requiring the presence of a stable β-turn conformation, like in the study of protein−protein interactions.

EXPERIMENTAL SECTION

Synthesis. The melting points of the compounds were determined in open capillaries and are uncorrected. High-quality infrared spectra (64 scans) were obtained at 2 cm−1 resolution using a 1 mm NaCl solution cell and a FT-infrared spectrometer. All spectra were obtained in 3 mM solutions in dry CH_2Cl_2 at 297 K. All compounds were dried in vacuo, and all of the sample preparations were performed in a nitrogen atmosphere. NMR spectra were recorded at 400 MHz (1H NMR) and at 100 MHz (13C NMR). The measurements were carried out in CD_3OD and in $CDCl_3$. The proton signals were assigned by gCOSY spectra. Chemical shifts are reported in δ values relative to thesolvent (CD_3OD or $CDCl_3$) peak.

(4S,5S)-4-(Hydroxymethyl)-5-methyloxazolidin-2-one (D-1). DThr-OMe (2.1 g, 12.6 mmol) was stirred in THF (15 mL) at room temperature until it was fully dissolved. Then triphosgene (3.9 g, 13.2mmol) was added, and the reaction was stirred and refluxed for 1 h in an apparatus equipped with refrigerator and a trap containing $CaCl_2$ and NaOH. Then the mixture was cooled to room temperature, and the solvent was removed in vacuo. The (4S,5S)-4-(carboxymethyl)-5-methyloxazolidin-2-one was obtained in 86% yield (1.72 g) and directly transformed in D1. Solid $NaBH_4$ (1.64 g, 11 mmol) was added to a stirred solution of (4S,5S)-4-(carboxymethyl)-5-methyloxazolidin-2-one (1.59 g, 10 mmol) in dry ethanol at 0 °C. After 5 min, the mixture was heated at room temperature and stirred for 1.5 h, and then a saturated aqueous solution of NH_4Cl (2.5 mL) was added and the mixture was stirred for additional 45 min. Then the mixture was filtered to eliminated the inorganic salts and concentrated in vacuo, leading to theformation of a waxy solid in 82% yield (1.08 g): $[\alpha]_D^{20} = -58.8$ (c =1.5, $CHCl_3$); IR (CH_2Cl_2, 3 Mm) ν 3611, 3452, 3280, 1760 cm−1; 1H NMR ($CDCl_3$, 400 MHz) δ 1.44 (3H, d, J = 7.2 Hz, Oxd-CH_3), 3.49−3.60 (2H, m, CHN-Oxd + CHNCHH), 3.65−3.79 (1H, m, CHN−CHH), 4.51 (1H, quintet, J = 5.6 Hz, CHO-Oxd), 6.73 (1H, bs, NH);13C NMR ($CDCl_3$, 100 MHz) δ 20.3, 60.9, 62.8, 75.6, 160.3. Anal. Calcd for $C_5H_9NO_3$: C, 45.80; H, 6.92; N, 10.68. Found: C, 45.78; H, 6.91; N, 10.70.

[(4S,5S)-5-Methyl-2-oxooxazolidin-4-yl]methyl Methylparatoluensulfonate (D-2). To a stirred solution of D-1 (1.6 g, 12.6 mmol)and (dimethylamino)pyridine (0.13 g, 1.1 mmol) in pyridine (12 mL) was added tosyl chloride (3.4 g, 17.7 mmol) at 0 °C, and stirring was maintained for 18 h at room temperature. After the end of the reaction, checked by TLC, CH_2Cl_2 (50 mL) was added, and the mixture was washed with brine (3 × 30 mL). The organic phase was dried over sodium sulfate and concentrated under low pressure. The product was obtained pure after silica gel chromatography (cyclohexane/ethyl acetate 80:20 → cyclohexane/
ethyl acetate 10:90 as eluant) in 74% overall yield as a white solid (2.66 g): mp = 95−98 °C; $[\alpha]_D^{20} = -32.2$ (c = 1.5, $CHCl_3$); IR (CH_2Cl_2, 3 Mm): ν 3441, 1767, 1365 cm−1; 1H NMR ($CDCl_3$, 400 MHz) δ 1.38 (3H, d, J = 6.0 Hz, Oxd-CH_3), 2.43 (3H, s, Ar−CH_3), 3.64 (1H, dt, J = 5.6, 5.3 Hz CHN-Oxd), 3.96 (2H, dd, J = 5.3, Hz,CH_2-Ts), 4.37 (1H, quintet, J = 5.6 Hz, CHO-Oxd), 6,40 (1H, bs, NH), 7.24 (2H, d, J = 8.4 Hz, Ar), 7.75 (2H, d, J = 8.4 Hz, Ar); 13CNMR ($CDCl_3$, 100 MHz) δ 20.4, 21.7, 57.6, 69.4, 75.3, 127.8, 128.1, 130.0 130.3, 132.0, 145.5, 158.7. Anal. Calcd for $C_{12}H_{15}NO_5S$: C, 50.52; H, 5.30; N, 4.91. Found: C, 50.55; H, 5.28; N, 4.94.

(4S,5S)- 4-(Azidomethyl)-5-methyloxazolidin-2-one (D-3). To a stirred solution of compound D-2 (2.63 g, 9.2 mmol) in dry DMF (15mL) was added sodium azide (0.66 g, 10.2 mmol). The mixture wasstirred under microwave irradiation at 150 W for 25 min. At the end of the reaction, as checked by TLC, ethyl acetate (40 mL) was added to the mixture, and the organic phase was washed with water and with a 1M aqueous solution of HCl. The organic layer was isolated, dried over sodium sulfate, and concentrated under low pressure. The product was obtained pure without any further purification in 79% yield (1.14 g) as a yellow oil: [α]20

D = −37.5 (c 0.9, CHCl3); IR (CH2Cl2, 3 Mm) ν 3440, 2120, 1764 cm−1; 1H NMR (CDCl3, 400 MHz) δ 1.44 (3H, d, J

= 6.4 Hz, Oxd-CH3), 3.44 (2H, ABX, JAB = 12.4 Hz, JAX = 5.2 Hz, JBX = 5.6 Hz, CH2−N3), 3.55 (1H, dd, J = 5.2, 12.0 Hz, CHN), 4.44 (1H, dq, J = 0.8, 6.8 Hz), 6.87 (1H, bs, NH); 13C NMR (CDCl3, 100 MHz) δ 20.4, 53.5, 58.4, 76.3, 159.2. Anal. Calcd for C5H8N4O2: C, 38.46; H,5.16; N, 35.88. Found: C, 38.42; H, 5.19; N, 35.85.

D-Oxd-Tri-COOBn (D-4). To a stirred solution of benzyl propiolate (0.25 g, 1.6 mmol) in dry acetonitrile (10 mL) were added
diisopropylethylamine (3.2 mmol, 0.56 mL), lutidine (3.2 mmol,0.37 mL), CuI (0.16 mmol, 0.03 g), and azide D-3 (1.6 mmol, 0.25 g) in this order at room temperature. Stirring was maintained for about 2 h at room temperature, and then, after the reaction was checked by TLC, the acetonitrile was removed under reduced pressure, replaced with ethyl acetate, and washed twice with brine (3 × 30 mL). The organic layer was isolated, dried over sodium sulfate, and concentrated under reduced pressure. The product was obtained pure after silica gel chromatography (cyclohexane/ethyl acetate 30:70 → ethyl acetate 100% as eluant) in 78% yield (0.39 g) as a white solid: mp = 165−166 °C; [α]20D = −52.0 (c 1.2, CHCl3); IR (CH2Cl2, 3 Mm): ν 3436,3284, 1765 cm−1; 1H NMR (CDCl3, 400 MHz) δ 1.36 (3H, d, J = 6.4 Hz, CHCH3), 3.95 (1H, m, CHN), 4.41−4.55 (3H, m, CHO + CH2CH), 5.38 (2H, AB, J = 12.8 Hz, CH2Ph), 7.03 (1H, bs, NH), 7.25−7.47 (5H, m, Ph), 8.11 (1H, s, CH-triazole); 13C NMR (CDCl3, 100 MHz) δ 20.2, 53.1, 58.5, 67.0, 75.7, 128.6, 128.7, 129.0, 135.2, 158.4, 160.3. Anal. Calcd for C15H16N4O4: C, 56.96; H, 5.10; N, 17.71. Found: C, 56.91; H, 5.14; N, 17.65.

Boc-L-Ala-D-Oxd-Tri-COOBn (5). A stirred solution of Boc-L-Ala-OH (0.09 g, 0.47 mmol) and HBTU (0.20 g, 0.52 mmol) in dry acetonitrile (20 mL) was stirred under nitrogen atmosphere for 10 min at room temperature. Then D-Oxd-Tri-OBn D-4 (0.150 g, 0.474 mmol) and DBU (0.141 mL, 0.948 mmol) in dry acetonitrile (10 mL) were added at room temperature. The solution was stirred for 2 h under nitrogen atmosphere, and then acetonitrile was removed under reduced pressure and replaced with ethyl acetate. The mixture was washed with brine (1 × 30 mL), 1 N aqueous HCl (1 × 30 mL), and with a concentrated solution of NaHCO3 (1 × 30 mL), dried over sodium sulfate and concentrated in vacuo. The product was obtained pure after silica gel chromatography (cyclohexane/ethyl acetate 30:70 → ethyl acetate 100% as eluant) as a white solid in 95% yield (0.22 g). Mp = 155−156 °C; [α]20D = −26.9; (c = 1.4, CHCl3); IR (CHCl3, 3mM): ν 3440, 1789, 1704 cm−1; 1H NMR (CDCl3, 400 MHz) δ 1.40 (3H, d, J = 7.6 Hz, CHCH3), 1.42 (9H, s, t-Bu), 1.43 (3H, d, J = 6.0 Hz, CHCH3), 4.44 (1H, q, J = 3.6 Hz, CHN), 4.75−4.80 (2H, m, CH2CH), 4.84 (1H, dq, J = 3.4, 5.6 Hz, CHO), 5.05 (1H, bs, NH), 5.27 (q, 1H, J = 6.8 Hz, CHAla), 5.41 (2H, AB, J = 13.6 Hz, CH2Ph), 7.28−7.49 (5H, m, Ph), 8.78 (1H, s, CH-triazole); 13C NMR (CDCl3, 100 MHz) δ 16.6, 20.5, 28.2, 49.2, 49.6, 59.7, 66.8, 73.5, 80.5, 128.3, 128.4, 128.5,

129.6, 135.5, 140.6, 151.3, 155.6, 160.2, 175.2. Anal. Calcd for C23H29N5O7: C, 56.67; H, 6.00; N, 14.37. Found: C, 56.70; H, 5.97; N, 14.35.

Boc-L-Ala-D-Oxd-Tri-COOH (6). Compound 5 (0.3 g, 0.61 mmol) was dissolved in MeOH (30 mL) under nitrogen. C/Pd (30 mg, 10% w/w) was added under nitrogen. A vacuum was created inside the flask using the vacuum line. The flask was then filled with hydrogen using a balloon (1 atm). The solution was stirred for 4 h under a hydrogen atmosphere. The product was obtained pure as an oil in 98% yield (0.24 g), after filtration through filter paper and concentration in vacuo: mp = 194 °C dec; [α]20D = −21.9 (c = 0.91, CHCl3); IR 3440, 1789, 1709, 1705, 1700 cm−1; 1H NMR (CD3OD, 400 MHz) δ 1.34 (3H, d, J = 6.0 Hz, CHCH3), 1.36 (3H, d, J = 6.8 Hz, CHCH3), 1.43 (9H, s, t-Bu), 4.51−4.58 (1H, m, CHN), 4.69−4.80 (3H, m, CH2CH + CHO), 5.16−5.28 (m, 1H, CH-Ala), 8.60 (1H, s, CH-triazole); 13C NMR (CD3OD, 100 MHz) δ 16.0, 19.2, 27.3, 49.2, 66.7, 74.2, 79.1,128.8, 142.6, 152.1, 156.4, 174.7. Anal. Calcd for C16H23N5O7: C, 48.36; H, 5.83; N, 17.62. Found: C, 48.40; H, 5.85; N, 17.59.

Boc-(L-Ala-D-Oxd-Tri-CO)2OBn (7). A solution of 5 (0.14 g, 0.287 mmol) and TFA (0.14 mL, 1.80 mmol) in dry methylene chloride (20mL) was stirred at room temperature for 4 h, then the volatiles were removed under reduced pressure and CF3COO− H3N+-L-Ala-D-Oxd-Tri-COOBn was obtained pure without further purification as a waxy solid. 1H NMR (CD3OD, 400 MHz) δ 1.40 (3H, d, J = 6.4 Hz, CHCH3), 1.53 (3H, d, J = 6.8 Hz, CHCH3), 4.62−4.67 (1H, m, CHAla), 4.74−5.05 (4H, m, CH2CH + CHO + CHN), 5.37 (2H, s, CH2Ph), 7.29−7.40 (5H, m, Ph), 8.66 (1H, s, CH-triazole). A solution of 6 (0.11 g, 0.287 mmol) and HATU (0.12 g, 0.32 mmol) in dry acetonitrile (20 mL) was stirred under nitrogen atmosphere for 10 min at room temperature. Then a mixture of the previously obtained CF3COO− H3N+-L-Ala-D-Oxd-Tri-COOBn (0.143 g, 0.287 mmol) and DIEA (0.17 mL, 1.02 mmol) in dry acetonitrile (10 mL) was added dropwise at room temperature. The solution was stirred for 50 min under nitrogen atmosphere, then acetonitrile was removed under reduced pressure and replaced with ethyl acetate. The mixture was washed with brine (1 × 30 mL), 1 N aqueous HCl (1 ×30 mL), and with a concentrated solution of NaHCO3 (1 × 30 mL), dried over sodium sulfate and concentrated in vacuo. The product was obtained pure after silica gel chromatography (c-Hex/ethyl acetate 30:70 → ethyl acetate 100% as eluant) in 70% overall yield (0.16 g), as a white solid: mp = 164 °C; [α]20D = +48.5 (c = 1.0, CHCl3); IR (CHCl3, 3 mM) ν 3414, 1790, 1711, 1676 cm−1; 1H NMR (CDCl3, 400 MHz) δ 1.37−1.48 (18H, m, CHCH3 Ala +2 × CHCH3 Oxd + t-Bu), 1.59 (3H, d, J = 7.2 Hz, CHCH3 Ala), 4.40−4.50 (2H, m, 2 ×CHN), 4.74−4.89 (6H, m, 2 × CH2CH + 2 × CHO), 5.21−5.31 (1H, m, CH-Ala), 5.41 (2H, s, CH2Ph), 5.52−5.61 (1H, m, CH-Ala), 7.28− 7.54 (6H, m, Ph + NH), 8.47 (1H, s, CH-triazole), 8.78 (1H, s, CHtriazole); 13C NMR (CDCl3, 100 MHz) δ 16.5, 20.6, 28.2, 28.3, 29.7, 30.9, 37.5, 48.2, 48.7, 49.3, 59.2, 59.7, 73.4, 73.7, 74.0, 80.4, 127.5, 128.2, 128.4, 129.7, 135.5, 140.6, 142.7, 151.3, 159.7, 160.2, 173.6, 175.0. Anal. Calcd for C34H42N10O11: C, 53.26; H, 5.52; N, 18.27. Found: C, 53.29; H, 5.50; N, 18.31.

Boc-(L-Ala-D-Oxd-Tri-CO)2−OH (8). For the synthetic procedure from 7 (0.77 g, 0.100 mmol), see the preparation of 6 given above (99% yield, 0.099 mmol, 0.67 g): mp = 200 °C; [α]20D = +20.5 (c = 1.0, CH2Cl2); IR (CH2Cl2, 3 mM) ν 3446, 3412, 1790, 1718, 1670 cm−1; 1H NMR (CD3OD, 400 MHz) δ 1.34−1.45 (18H, m, CHCH3Ala +2 × CHCH3 Oxd + t-Bu), 1.50 (3H, d, J

= 6.4 Hz, CHCH3 Ala), 4.54−4.67 (2H, m, 2 × CHN), 4.74−4.95 (6H, m, 2 × CH2CH + 2 × CHO), 5.20 (m, 1H, CH-Ala), 5.59 (m, 1H, CH-Ala), 8.47 (1H, s, CH-triazole), 8.78 (1H, s, CH-triazole); 13C NMR (CD3OD, 100 MHz) δ 15.5, 15.6, 16.2, 27.3, 48.5, 49.2, 49.6, 51.2, 51.5, 52.4, 58.4, 59.6, 74.4, 75.9, 79.3, 127.8, 129.6, 142.2, 152.0, 152.1, 152.1, 156.4, 160.39, 160.5, 173.0, 173.2, 174.7. Anal. Calcd for C27H36N10O11: C, 47.93; H, 5.36; N, 20.70. Found: C, 47.88; H, 5.41; N, 20.74.

Boc-(L-Ala-D-Oxd-Tri-CO)3-OBn (9). A solution of 5 (0.049 g, 0.100 mmol) and TFA (0.14 mL, 1.80 mmol) in dry methylene chloride (20 mL) was stirred at room temperature for 4 h, and then the volatiles were removed under reduced pressure and CF3COO− H3N+-L-Ala-DThe Oxd-Tri-COOBn was obtained pure without further purification as a waxy solid. A solution of 8 (0.068 g, 0.100 mmol) and HATU (0.042 g, 0.11 mmol) in dry acetonitrile (20 mL) was stirred under nitrogen atmosphere for 10 min at room temperature. Then a mixture of the previously obtained CF3COO− H3N+-L-Ala-D-Oxd-Tri-COOBn and DIEA (0.04 mL, 0.3 mmol) in dry acetonitrile (10 mL) was added dropwise at room temperature. The solution was stirred for 50 min under nitrogen atmosphere, and then acetonitrile was removed under reduced pressure and replaced with ethyl acetate. The mixture was washed with brine (1 × 30 mL), 1 N aqueous HCl (1 × 30 mL), and a concentrated solution of NaHCO3 (1 × 30 mL), dried over sodium
sulfate, and concentrated in vacuo. The product was obtained pure after silica gel chromatography (c-Hex/ethyl acetate 10:90 → ethyl acetate 100% as eluant) in 51% yield (54 mg), as a white solid: mp =194 °C; [α]20D = +69.0 (c = 0.97, CH2Cl2); IR (CH2Cl2, 3 mM) ν 3446, 3412, 1790, 1718, 1670 cm−1; 1H NMR (CDCl3, 400 MHz) δ 1.38 (3H, d, J = 7.0 Hz, CH3 Ala), 1.38 (3H, d, J = 7.0 Hz, CH3 Oxd), 1.39 (9H, s, t-Bu), 1.43 (3H, d, J = 6.8 Hz, CH3 Oxd), 1.46 (3H, d, J =7.2 Hz, CH3 Oxd), 4.41−4.52 (3H, m, 3 × CHN), 4.65−4.90 (9H, m, 3 × CHO + 3 × CH2CH), 5.17 (1H, d, J = 6.4 Hz, NH), 5.28 (1H, q, J= 6.4 Hz, CH Ala), 4.32−5.42 (2H, m, CH2Ph), 5.52 (1H, m, CH Ala), 5.56 (1H, m, CH Ala), 7.29−7.39 (3H, m, Ph), 7.41−7.49 (2H, m, Ph), 7.57 (1H, d, J = 5.6 Hz, NH), 7.62 (1H, d, J = 5.6 Hz, NH), 8.50 (1H, s, CH-triazole), 8.64 (1H, s, CH-triazole), 8.75 (1H, s, CHtriazole); 13C NMR (CDCl3, 100 MHz) δ 16.2, 16.6, 20.6, 28.2, 48.6, 48.8, 49.5, 59.6, 59.7, 59.8, 66.8, 73.9, 80.4, 127.8, 128.3, 128.5, 129.8, 135.5, 142.6, 151.3, 151.5, 155.9, 159.8, 173.6, 177.8. Anal. Calcd for C45H55N15O15: C, 51.67; H, 5.30; N, 20.09. Found: C, 51.72; H, 5.28;
N, 20.11.

Boc-(L-Ala-D-Oxd-Tri-CO)3-OH (10). For the synthetic procedure from 9 (0.05 mmol, 52 mg), see the preparation of 6 given above (99% yield, 0.049 mmol, 47 mg): mp = 206 °C; [α]20 D = +120.0 (c = 0.90, CH2Cl2); IR (CH2Cl2, 3 mM) ν 3687, 3600, 3411, 1790, 1713, 1674, 1606, 1575, 1505 cm−1; 1H NMR (CDCl3, 400 MHz) δ 1.22−1.62 (27H, m, 3 × CH3 Ala + 3 × CH3 Oxd + t-Bu), 4.50−4.68 (3H, m, 3 × CHN), 4.69−4.99 (9H, m, 3 × CHO + 3 × CH2CH), 5.14−5.28 (1H, m, CH-Ala), 5.57−5.70 (2H, m, 2 × CH-Ala), 8.68 (1H, s, CH-triazole), 8.74 (1H, s, CH-triazole), 8.77 (1H, s, CH-triazole); 13C NMR (CDCl3, 100 MHz) δ 15.7, 19.0, 27.3, 36.0, 37.6, 49.3, 59.6, 66.7, 74.1, 74.4, 79.2, 127.9, 142.2, 152.0, 156.5, 160.6, 173.4, 174.7. Anal. Calcd for C38H49N15O15: C, 47.75; H, 5.17; N, 21.98. Found: C, 47.70; H, 5.15; N, 22.02.

L-Oxd-Tri-COOBn (L-4). For the synthetic procedure from L-3 (1.6 mmol, 0.25 g), see the preparation of D-4 given above (78% yield, 1.25 mmol, 0.39 g): mp = 167 °C; [α]20D = +53.0 (c 1.6, CHCl3); IR (CH2Cl2, 3 Mm) ν 3436, 3284, 1765 cm−1; 1H NMR (CDCl3, 400 MHz) δ 1.38 (3H, d, J = 6.4 Hz, CHCH3), 3.95 (1H, m, CHN), 4.41−4.55 (3H, m, CHO + CH2CH), 5.31

(2H, AB, J = 12.8 Hz, CH2Ph), 7.03 (1H, bs, NH), 7.25−7.47 (5H, m, Ph), 8.26 (1H, s, CH-triazole); 13C NMR (CDCl3, 100 MHz) δ 20.2, 53.1, 58.5, 67.0, 75.7, 128.6, 128.7, 129.0, 135.2, 158.4, 160.3. Anal. Calcd for C15H16N4O4: C, 56.96; H, 5.10; N, 17.71. Found: C, 56.91; H, 5.14; N, 17.65.

Boc-L-Ala-L-Oxd-Tri-COOBn (11). For the synthetic procedure from L-4 (1.2 mmol, 0.38 g), see the preparation of 5 given above (71% yield, 0.85 mmol, 0.41 g): mp = 117−118 °C; [α]20D = −38.0 (c 0.8, CH3OH); IR (CH2Cl2, 3 Mm) ν 3436, 1780, 1740, 1708 cm−1; 1H NMR (CDCl3, 400 MHz) δ 1.38 (3H, d, J = 6.8 Hz, CHCH3), 1.48 (12H, m, CH3−Ala + t-Bu), 4.38 (1H, m, CHN), 4.65 (1H, d, J = 3.6, 6.4 Hz, CHO), 4.80 (2H, m, CH2CH), 5.13 (1H, m, NH-Boc), 5.25 (1H, m, CH-Ala), 5.40 (2H, s, CH2Ph), 7.25−7.43 (5H, m, Ph), 8.10 (1H, s, CH-triazole). 13C NMR (CDCl3, 100 MHz) δ 15.2, 18.1, 20.2, 28.3, 49.6, 59.6, 67.1, 74.2, 128.5, 128.6, 135.1, 140.2, 151.3, 160.0, 175.0. Anal. Calcd for C23H29N5O7: C, 56.67; H, 6.00; N, 14.37. Found: C, 56.65; H, 5.99; N, 14.40.

Boc-L-Ala-L-Oxd-Tri-COOH (12). For the synthetic procedure from 11 (0.80 mmol, 0.32 g), see the preparation of 6 given above (99% yield, 0.79 mmol, 0.31 g): mp = 180 °C dec; [α]20D = −48.7 (c = 2.5, CHCl3); IR (nujol): ν 3442, 3138, 1785, 1731, 1706, 1701, 1685 cm−1; 1H NMR (CD3OD, 400 MHz) δ 1.32 (3H, d, J = 6.0 Hz, CHCH3), 1.40 (9H, s, t-Bu), 1.43 (3H, d, J = 6.8 Hz, CHCH3), 4.55−4.59 (1H, m, CHN), 4.70−4.82 (2H, m, CH2CH), 4.93 (m, 1H, CHO), 5.10−5.16 (m, 1H, CH-Ala), 8.32 (1H, s, CH-triazole); 13C NMR (CD3OD, 100 MHz) δ 16.2, 18.9, 27.3, 29.3, 35.8, 49.7, 59.25 73.9, 74.2, 79.1, 129.1, 142.6, 152.1, 156.5, 174.7. Anal. Calcd for C16H23N5O7: C, 48.36; H, 5.83; N, 17.62. Found: C, 48.39; H, 5.80; N, 17.57.

Boc-(L-Ala-L-Oxd-Tri-CO)2-OBn (13). A solution of 11 (0.14 g, 0.287 mmol) and TFA (0.14 mL, 1.80 mmol) in dry methylene chloride (20 mL) was stirred at room temperature for 4 h, and then the volatiles were removed under reduced pressure and CF3COO− H3N+-L-Ala-L-Oxd-Tri-COOBn was obtained pure without further purification as a waxy solid: 1H NMR (CD3OD, 400 MHz) δ 1.44 (3H, d, J = 6.4 Hz, CHCH3), 1.52 (3H, d, J = 7.2 Hz, CHCH3), 4.64 (1H, q, J = 3.8 Hz, CH-Ala), 4.73−4.81 (2H, m, CHHCH + CHN), 4.86−4.93 (1H, m, CHO), 4.98 (1H, dd, J = 4.0, 14.8 Hz, CHHCH), 5.35 (2H, AB, J = 13.2 Hz, CH2Ph), 7.29−7.47 (5H, m, Ph), 8.64 (1H,s, CH-triazole). A solution of 12 (0.113 g, 0.287 mmol) and HATU (0.12 g, 0.32 mmol) in dry acetonitrile (20 mL) was stirred under nitrogen atmosphere for 10 min at room temperature. Then a mixture of the previously obtained CF3COO− H3N+-L-Ala-D-Oxd-Tri-COOBn and DIEA (0.17 mL, 1.02 mmol) in dry acetonitrile (10 mL) was added dropwise at room temperature. The solution was stirred for 50 min under nitrogen atmosphere, and then acetonitrile was removed under reduced pressure and replaced with ethyl acetate. The mixture was washed with brine (1 × 30 mL), 1 N aqueous HCl (1 × 30 mL), and a concentrated solution of NaHCO3 (1 × 30 mL), dried over sodium sulfate, and concentrated in vacuo. The product was obtained pure after silica gel chromatography (c-Hex/ethyl acetate 30:70 → ethyl acetate 100% as eluant) in 70% overall yield (0.20 mmol, 0.15 g), as a white solid: mp = 110 °C; [α]20D = −60.5; IR (CHCl3, 3 Mm) ν 34383434, 3410, 1674, 1791, 1743, 1710 cm−1; 1H NMR (CD3OD, 400 MHz) δ 1.31 (3H, d, J = 7.2 Hz), 1.41 (9H, s, t-Bu), 1.43 (15H, m, CH3−Oxd), 1.46 (3H, d, J = 8 Hz), 4.51−4.65 (3H, m, CHN-Oxd), 4.69−4.80 (4H, m, CHO-Oxd), 5.11 (1H, q, J = 6.8 Hz), 5.36 (2H, s), 5.55 (1H, q, J = 7.2 Hz), 7.27−7.47 (5H, m), 8.37 (1H, s, CHtriazole), 8.58 (1H, s, CH-

triazole); 13C (CD3OD, 100 MHz) δ 17.6, 20.3, 28.7, 29.5, 38.9, 48.3, 49.0, 49.6, 50.3, 51.0, 53.9, 59.7, 60.6, 67.9, 75.8, 77.3, 80.6, 129.0, 129.6, 131.0, 137.0, 140.7, 143.4, 153.5, 157.9, 161.6, 174.5, 175.8. Anal. Calcd for C34H42N10O11: C, 53.26; H, 5.52; N, 18.27. Found: C, 53.22; H, 5.48; N, 18.26.

Boc-(L-Ala-L-Oxd-Tri-CO)2-OH (14). For the synthetic procedure from 13 (0.20 mmol, 0.15 g), see the preparation of 6 given above (99% yield, 0.19 mmol, 0.13 g): mp = 200 °C; [α]20 D = −60.9 (c = 1.0, CH3OH); IR (nujol) ν 3373, 3144, 1781, 1744, 1707, 1663, 1577, 1507 cm−1; 1H NMR (CD3OD, 400 MHz) δ 1.26−1.51 (21H, m, 2 × CHCH3-Ala +2 × CHCH3-Oxd + t-Bu), 4.52−4.82 (8H, m, 2 × CHN + 2 × CHO + 2 × CH2CH) 5.11 (1H, q, J = 6.8 Hz, CH-Ala), 5.57 (1H, q, J = 6.8 Hz, CH-Ala), 8.28 (1H, s, CH-triazole), 8.40 (1H, s, CH-triazole); 13C NMR (CD3OD, 100 MHz) δ 16.2, 16.3, 19−0 27.3, 48.9, 49.6, 52.3, 52.4, 58.3, 58.4, 58.5, 59.6, 74.4, 75.9, 79.2, 127.1, 127.6, 129.2, 142.0, 142.2, 152.1, 156.5, 159.3, 160.4, 173.0, 173.0, 173.2, 174.4. Anal. Calcd for C27H36N10O11: C, 47.93; H, 5.36; N, 20.70. Found: C, 47.94; H, 5.38; N, 20.73.

Boc-(L-Ala-L-Oxd-Tri-CO)3-OBn (15). For the synthetic procedure from 11 (0.15 mmol, 0.10 g), see the preparation of 9 given above (40% yield, 0.04 mmol, 42 mg): mp = 108 °C; [α]20 D = −17.5; IR (CHCl3, 3 Mm) ν 3447, 3433, 3410, 1789, 1772, 1749, 1712, 1676 cm−1; 1H NMR: (CD3OD): δ 1.31 (3H, d, J = 6,8 Hz, CH3−Ala), 1.41 (9H, s, t-Bu), 1.48 (3H, d, J = 6 Hz, CH3−Ala), 1.49 (3H, d, J = 7.6 Hz, CH3−Ala), 4.50−4.60 (6H, m, 3 × CHO-Oxd + 3 × CHN-Oxd), 5.10 (1H, d, J = 6.8 Hz, CH-Ala), 5.36 (2H, s), 5.56 (1H, d, J = 6 Hz), 5.59 (1H, d, J = 7.6 Hz), 7.41−7.47 (2H, m), 7.28−7.40 (3H, m), 8.37 (1H, s, CH-triazole), 8.40 (1H, s, CH-triazole), 8.59 (1H, s, CHtriazole); 13C NMR (CD3OD, 100 MHz) δ 18.7, 21.4, 31.7, 49.4, 49.6, 49.8, 50.0, 50.3, 50.5, 50.7, 51.4, 52.1, 54.9, 60.9, 61.8, 69.0, 77.0, 78.4, 81.8, 130.1, 130.7, 131.9, 132.3, 138.2, 141.8, 144.7, 154.6, 159.0, 162.9, 175.6. Anal. Calcd for C45H55N15O15: C, 51.67; H, 5.30; N, 20.09. Found: C, 51.66; H, 5.27; N, 20.05.

Boc-(L-Ala-L-Oxd-Tri-CO)3-OH (16). For the synthetic procedure from 15 (0.04 mmol, 42 mg), see the preparation of 6 given above (99% yield, 0.39 mmol, 38 mg): mp = 155 °C; [α]20 D = −23.2 (c = 0.50, CH3OH); IR (nujol): ν 3335, 1748, 1735, 1684, 1653, 1617, 1577, 1559, 1507 cm−1; 1H NMR (CD3OD, 400 MHz) δ 1.13−1.67 (27H, m, 3 × CH3 Ala + 3 × CH3 Oxd + t-Bu), 3.92−4.01 (3H, m, 3× CHN), 4.54−4.68 (10H, m, 3 × CHO + 3 × CH2CH + CH-Ala), 4.95−5.05 (2H, m, 2 × CH-Ala), 8.68 (1H, s, CH-triazole), 8.74 (1H, s, CH-triazole), 8.77 (1H, s, CH-triazole); 13C NMR (CD3OD, 100 MHz) δ 16.1, 19.0, 29.3, 36.0, 37.6, 51.5, 52.2, 52.3, 58.4, 58.5, 75.9, 126.5, 127.1, 142.2, 159.3, 160.6, 172.9. Anal. Calcd for C38H49N15O15: C, 47.75; H, 5.17; N, 21.98. Found: C, 47.79; H, 5.19; N, 21.96.

ECD Spectroscopy. Measurements were performed in a cylindrical, fused quartz cell (1 mm path length). Each pseudopeptide was dissolved in MeOH/H2O 8:2 v/v at 0.1−1 mM concentration. Metal-binding experiments were performed by adding aliquots of a 65 mM CuSO4 solution in MeOH/H2O 8:2 v/v. Ligand competition experiments were performed by adding aliquots of a 0.1 M EDTA solution in H2O.

UV−vis Spectroscopy. Electronic absorption spectra in the absence and presence of Cu2+ were recorded at RT on a doublebeam spectrophotometer, in quartz cells (1 cm-path length). Metal binding experiments were performed by adding aliquots of a 65 mM CuSO4 solution in

MeOH/H2O 8:2 v/v 0.696 mM pseudopeptides solutions in MeOH/H2O 8:2 v/v. The dissociation constant (KD) of the ligand−metal complexes was determined by complexometric titration according to the protocol described by Ferrari et al.28

X-ray Crystallography. Structural investigations by single-crystal X-ray crystallography on 5 and 7·0.5C6H6 were carried out on a diffractometer equipped with a Mo Kα generator, area detector, and Kryo-Flex liquid-nitrogen cryostat. Crystals were grown from benzene (5) or from benzene/methyl tert-butyl ether 1:1 v/v (7) via vapor diffusion over a Nujol trap. The very long needles so obtained were cut to a proper size using a razor blade, fixed on the tip of a glass capillary with vacuum grease and transferred to the cold nitrogen stream for data collection at 150(2) K. Evaluation of the crystal quality and determination of unit cell parameters were based on 60 preliminary frames collected using ω scans. Data collection was based on ω or ϕ scans (0.4°) and was extended up to 2θ = 54°. Data integration, reduction, and correction for absorption were based on standard methods. The structures were solved by direct-methods program SIR9229 and refined on F02 by SHELXL-9730 using the WINGX v2013.3 package.31 All non-hydrogen atoms were refined anisotropically (unless otherwise stated), while hydrogen atoms were treated isotropically. In 5, an idealized geometry was assigned to methyl hydrogens, but the torsion angle was allowed to refine freely (AFIX 137 instruction). Their displacement parameter was constrained to be 1.5 times larger than the Uiso of the parent C atom. Phenyl hydrogen atoms were subject to unconstrained refinement, while methylene hydrogens on C1 were forced to have the same U value. The remaining H atoms were treated with a common displacement parameter. The absolute structure of 5 could not be reliably determined with Mo Kα radiation and was chosen to give S configuration at C12, C13, and C17. In 7·0.5C6H6, the terminal phenyl ring was found disordered over two positions with 0.70:0.30 occupancies. The two components were restrained to have same geometry and to approach mm2 symmetry and were refined isotropically with identical U values for corresponding atoms. An idealized geometry was assigned to methyl hydrogens, whose displacement parameter was constrained to be 1.5 times larger than the Uiso of the parent C atom. Torsion angle was however allowed to refine freely (AFIX 137 instruction), except for Boc methyls (AFIX 33). For the remaining hydrogen atoms two common U values were introduced after inspection of the Uiso parameters of the attached C orN atoms. Triazole CH hydrogens were set on the N−C−C bisector but the C−H distance was allowed to refine (AFIX 44) and restrained to be similar within 0.02 Å in the two moieties. The amide N−H distances where also restrained to 0.880(15) Å, while C−H distances for tertiary hydrogens on C17 and C28 where forced to be similar within 0.02 Å. After localization of all atoms in the trimer, the unit cell contained 254 Å3 of potentially solvent-accessible void mainly centered at (0.5, 0.0, 0.0). Electron density residuals (<0.8 e Å3) arranged in an approximately planar fashion were fitted to a half-occupancy benzene molecule, as required for reasonable intermolecular contacts, affording final indices wR2 = 0.1504 (on all data) and R1 = 0.0534 (on data with I > 2σ(I)). Alternatively, data were treated using SQUEEZE routine in PLATON (V-290610) software to remove the contribution from disordered solvent.32 Final refinement on corrected data gave wR2 = 0.1348 (on all data) and R1 = 0.0497 (on data with I > 2σ(I)) with only slight improvement of bond precision (from 0.0051 to 0.0045 Å for C−C bonds). For this reason, the former approach was preferred. The absolute structure of 7·0.5C6H6 could not be reliably determined with Mo Kα radiation and was chosen to give the S configuration at C12, C13, C17, C23, C24, and C28. CCDC 997293−997294 contain the supplementary crystallographic data for this paper. These data can be obtained free of charge from the Cambridge Crystallographic Data Centre via www.ccdc.cam.ac.uk/data_request/cif.

EPR Spectroscopy. X-band EPR spectra of the Cu2+-peptidomimetic complexes were recorded at 77 K. Instrumental settings: frequency 9.492 GHz; microwave power 5.078 mW modulation amplitude 2.072 G; modulation frequency 100 MHz; magnetic field range 2300−4000 G;. time constant 163.8 ms; conversion time 163.8 ms. Aliquots of a 65 mM CuSO4 solution in MeOH/H2O 8:2 v/v were added to 1−5 mM pseudopeptides solutions in MeOH/H2O 8:2 v/v. Ligand competition experiments were performed by adding aliquots of a 0.1 M EDTA solution in H2O. Spectral simulations were performed with the EPRSim32 software.33

Molecular Dynamics Simulations. Molecular dynamics simulations were carried out with the AMBER 11.0 suite of programs.34 The peptide is parametrized using AMBER10 force field34 for the L-Ala residues and GAFF (general AMBER force field) force field35 for the L(D)-Oxd-Tri residues (the standard RESP procedure is carried out to assign charges to atoms by Antechamber).36 A linear conformation of the peptide was built and immersed in a solvent box of explicit methanol molecules. Periodic boundary conditions were used. An equilibration protocol consisting of four individual steps was applied, resulting in an unconstrained well-tempered NPT ensemble at target conditions. A Langevin thermostat was used to set a constant temperature at 300 K and 1 atm. Particle Mesh Ewald37 summation was used throughout (cut off radius of 10 Å for the direct space sum). Bonds involving H atoms were constrained using the SHAKEalgorithm,38 and a time step of 2 fs was applied in all runs. Overall sampling time for MD production was 1 μs. Snapshot structures were saved into individual trajectory files every 5000 time steps, that is, every 10 ps of molecular dynamics, for a total of 100000 snapshots. MD simulations were carried out using pmemd.35 VMD was used to visualize the trajectory.39

Two-dimensional free-energy profiles for the peptide in explicit solvent were obtained as a function of PCA1 and PCA2. The program "ptraj"34 in the AMBER package was used in the PCA. The values are given in kcal mol−1. The energy landscape of the peptide is visualized by means of free-energy functions, which are projected as contour lines onto a two-dimensional space formed by the PCA1/PCA2 axes. These coordinates are derived from a principal component analysis.25a The free-energy change associated with the passage between two different states of a system in thermodynamic equilibrium is given by $\Delta G = -RT (\ln p1/p2)$. Here, R is the ideal gas constant, T is the absolute temperature, and pi is the probability of finding the system in state i. The two-dimensional space defined by the PCA1 and PCA2 axes has been divided into a grid and the free energy has been calculated for each bin of the grid on the basis of the previous equation. The whole set of G values was shifted in such a way that the lowest value of the free energy surface corresponds to zero. Thus, the reported ΔG value represent the transfer free energies with respect to the bin that has been set to zero. To obtain the p values, the trajectory at ambient temperature was projected onto the PCA1/PCA2 space, and p corresponds to the number of times the trajectory "visits" a given bin.

ACKNOWLEDGMENTS

We thank the Italian "Ministero dell'Istruzione, dell'Universita e della Ricerca" (MIUR) (program PRIN 2010NRREPL_009) and "Consorzio Spinner Regione Emilia Romagna" for financial support.

REFERENCES

(1) Hill, D. J.; Mio, M. J.; Prince, R. B.; Hughes, T. S.; Moore, J. S. Chem. Rev. 2001, 101, 3893−4011. (b) Hecht, S.; Huc, I. Foldamers: Structure, Properties, and Applications; Wiley-VCH: Weinheim, 2007.

(2) Gellman, S. H. Acc. Chem. Res. 1998, 31, 173−180.

p, F. Chem. Soc. Rev. 2012, 41, 687−702. (b) Cubberley, M. S.; Iverson, B. L. Curr. Opin. Chem. Biol. 2001, 5, 650−653. (c) Seebach, D.; Beck, A. K.; Bierbaum, D. J. Chem. Biodivers. 2004, 1, 1111−1239. (d) Sanford, A.; Yamato, K.; Yang, X. W.; Yuan, L. H.; Han, Y. H.; Gong, B. Eur. J. Biochem. 2004, 271, 1416−1425. (e) Cheng, R. P. Curr. Opin. Struct. Biol. 2004, 14, 512− 520. (f) Balbo Block, M. A.; Kaiser, C.; Khan, A.; Hecht, S. Top. Curr. Chem. 2005, 245, 89−150. (g) Goodman, C. M.; Choi, S.; Shandler, S.; DeGrado, W. F. Nat. Chem. Biol. 2007, 3, 252−262. (h) Bautista, A. D.; Craig, C. J.; Harker, E. A.; Schepartz, A. Curr. Op. Chem. Biol. 2007, 11, 685−692. (i) Smaldone, R. A.; Moore, J. S. Chem.□Eur. J. 2008, 14, 2650−2657. (j) Guichard, G.; Huc, I. Chem. Commun. 2011,47, 5933−5941.

(4) Tomasini, C.; Angelici, G.; Castellucci, N. Eur. J. Org. Chem. 2011, 3648−3669.

(5) (a) Tomasini, C.; Villa, M. Tetrahedron Lett. 2001, 42, 5211−5214. (b) Bernardi, F.; Garavelli, M.; Scatizzi, M.; Tomasini, C.; Trigari, V.; Crisma, M.; Formaggio, F.; Peggion, C.; Toniolo, C. Chem.□Eur. J. 2002, 8, 2516−2525.

(6) Tomasini, C.; Luppi, G.; Monari, M. J. Am. Chem. Soc. 2006, 128, 2410−2420.

(7) (a) Sharma, G. V. M; Babu, B. S.; Chatterjee, D.; Ramakrishna, K. V. S.; Kunwar, A. C.; Schramm, P.; Hofmann, H.-J. J. Org. Chem. 2009, 74, 6703−6713.

(8) (a) Hayen, A.; Schmitt, M. A.; Nagassa, N.; Thomson, K. A.; Gellman, S. H. Angew. Chem., Int. Ed. 2004, 43, 505−510. (b) De Pol, S.; Zorn, C.; Klein, C. D.; Zerbe, O.; Reiser, O. Angew. Chem., Int. Ed. 2004, 43, 511−514. (c) Seebach, D.; Jaun, B.; Sebesta, R.; Mathad, R. I.; Flogel, O.; Limbach, M.; Sellner, H.; Cottens, S. Helv. Chim. Acta 2006, 89, 1801−1825. (d) Baldauf, C.; Gunther, R.; Hofmann, H.-J. Biopolymers 2006, 84, 408−413. (e) Sharma, G. V. M; Nagendar, P.; Jayaprakash, P.; Krishna, P. R.; Ramakrishna, K. V. S.; Kunwar, A. C. Angew. Chem., Int. Ed. 2005, 44, 5878−5882. (f) Choi, S. H.; Guzei, I. A.; Gellman, S. H. J. Am. Chem. Soc. 2008, 129, 13780−13781. (g) Prabhakaran, P.; Kale, S. S.; Puranik, V. G.; Rajamohanan, P. R.; Chetina, O.; Howard, J. A. K.; Hofmann, H.-J.; Sanjayan, G. J. J. Am. Chem. Soc. 2008, 130, 17743−17754. (h) Celis, S.; Gorrea, E.; Nolis, o, R. M. Org. Biomol. Chem. 2012, 10, 861−868. (i) Pilsl, L. K. A.; Reiser, O. Amino Acids 2011, 41, 709−718.

(9) (a) Price, J. L.; Horne, W. S.; Gellman, S. H. J. Am. Chem. Soc. 2007, 129, 6376−6377. (b) Seebach, D.; Gardiner, J. Acc. Chem. Res. 2008, 41, 1366−1375. (c) David, R.; Gunther, R.; Baumann, L.; Luhmann, T.; Seebach, D.; Hofmann, H.-J; Beck-Sickinger, A. G. J. Am. Chem. Soc. 2008, 130, 15311−15317.

(10) (a) Sharma, G. V. M; Jadhav, V. B.; Ramakrishna, K. V. S.; Jayaprakash, P.; Narsimulu, K.; Subash, V.; Kunwar, A. C. J. Am. Chem. Soc. 2006, 128, 14657−14668. (b) Baldauf, C.; Gunther, R.; Hofmann, H.-J. J. Org. Chem. 2006, 71, 1200−1208. (c) Chatterjee, S.; Vasudev, P. G.; Ragothama, S.; Shamala, N.; Balaram, P. Biopolymers 2008, 90,759−771. (d) Vasudev, P. G.; Chatterjee, S.; Ananda, K.; Shamala, N.; Balaram, P. Angew. Chem., Int. Ed. 2008, 47, 6430−6432. (e) Sharma,
G. V. M; Babu, B. S.; Ramakrishna, K. V. S.; Nagendar, P.; Kunwar, A. C.; Schramm, P.; Baldauf, C.; Hofmann, H.-J. Chem.□Eur. J. 2009, 15, 5552−5566. (f) Saludes, J. P.; Ames, J. B.; Gervay-Hague, J. J. Am.Chem. Soc. 2009, 131, 5495−5505.

(11) Castellucci, N.; Tomasini, C. Eur. J. Org. Chem. 2013, 3567−3573.

(12) Angelo, N. G.; Arora, P. S. J. Org. Chem. 2007, 72, 7963−7967.

(13) Brik, A.; Alexandratos, J.; Lin, Y.-C.; Elder, J. H.; Olson, A. J.; Wlodawer, A.; Goodsell, D. S.; Wong, C.-H. ChemBioChem 2005, 6, 1167−1169.

(14) (a) Wu, C.-F.; Li, Z.-M.; Xu, X.-N.; Zhao, Z.-X.; Zhao, X.; Wang, R.-X.; Li, Z.-T. Chem.□Eur. J. 2014, 20, 1418−1426. (b) Angelo, N. G.; Arora, P. S. J. Org. Chem. 2007, 72, 7963−7967. (c) You, L.-Y.; Chen, S.-G.; Zhao, X.; Liu, Y.; Lan, W.-X.; Zhang, Y.; Lu, H.-J.; Cao, C.-Y.; Li, Z.-T. Angew. Chem., Int. Ed. 2012, 51, 1657−1661. (d) Juwarker, H.; Lenhardt, J. M.; Pham, D. M.; Craig, S. L. Angew. Chem., Int. Ed. 2008, 47, 3740−3743. (e) Angelo, N. G.; Arora, P. S. J. Am. Chem. Soc. 2005, 127, 17134−17135.

(15) Yuan-Yuan, Liu J. Coord. Chem. 2007, 60, 2597−2605.
- - uelas-Zahínos, E.; Cumbrera, F. L.; Ortiz, A. L.; Barros-García, F. J.; Rodríguez, A. B. Inorg. Chim. Acta 2011, 365, 282−289.
(17) Nicoll, A. J.; Miller, D. J.; Futterer, K.; Ravelli, R.; Allemann, R. K. J. Am. Chem. Soc. 2006, 128, 9187−9193.
(18) (a) Tornoe, C. W.; Christensen, C.; Meldal, M. J. Org. Chem. 2002, 67, 3057−3064. (b) Zhang, L.; Chen, X. G.; Xue, P.; Sun, H. H. Y.; Williams, I. D.; Sharpless, K. B.; Fokin, V. V.; Jia, G. C. J. Am. Chem. Soc. 2005, 127, 15998−15999.
(19) Lemen, G. S.; Wolfe, J. P. Org. Lett. 2010, 12, 2322−2325.
(20) Hu, T.-S.; Tannert, R.; Arndt, H.-D.; Waldmann, H. Chem. Commun. 2007, 38, 3942−3944.
(21) (a) Belvisi, L.; Gennari, C.; Mielgo, A.; Potenza, D.; Scolastico, C. Eur. J. Org. Chem. 1999, 389−400. (b) Yang, J.; Gellman, S. H. J. Am. Chem. Soc. 1998, 120, 9090−9091. (c) Jones, I. G.; Jones, W. North, M. J. Org. Chem. 1998, 63, 1505−1513. (d) Toniolo, C.; Benedetti, E. CRC Crit. Rev. Biochem. 1980, 9, 1−44. (e) Imperiali, B.; Moats, R. A.; Fisher, S. L.; Prins, T. J. J. Am. Chem. Soc. 1992, 114, 3182−3188.
(22) Pokorski, J. K.; Miller Jenkins, L. M.; Feng, H.; Durell, S. R.; Bai, Y.; Appella, D. H. Org. Lett. 2007, 9, 2381−2388.
(23) Toniolo, C.; Formaggio, F.; Tonion, S.; Broxterman, Q. B.; Kaptein, B.; Huang, R.; Setnicka, V.; Keiderling, T. A.; McColl, I. H.; Hecht, L.; Barron, L. D. Biopolymers 2004, 75, 32−45.
(24) Farrugia, L. J. J. Appl. Crystallogr. 1997, 30, 565−565.
(25) (a) Daidone, I.; Amadei, A. WIREs Comput. Mol. Sci. 2012, 2, 762−770. (b) Fermani, S.; Trivelli, X.; Sparla, F.; Thumiger, A.; Calvaresi, M.; Marri, L.; Falini, G.; Zerbetto, F.; Trost, P. J. Biol. Chem.2012, 287, 21372−21383.
(26) (a) Sakaguchi, U.; Addison, A. W. J. Chem. Soc., Dalton Trans. 1978, 601−608. (b) Romanowski, S. M.; Tormena, F.; dos Santos, V.A.; Hermann, M.; Mangrich, A. S. J. Braz. Chem. Soc. 2004, 897−903.
(27) Hathaway, B. J. J. Chem. Soc., Dalton Trans. 1971, 1196−1199.
(28) Ferrari, R. P.; Ghibaudi, E. M.; Traversa, S.; Laurenti, E.; De Gioia, L.; Salmona, M. J. Inorg. Biochem. 1997, 68, 17−26.
(29) Altomare, A.; Cascarano, G.; Giacovazzo, C.; Guagliardi, A. J. Appl. Crystallogr. 1993, 26, 343−350.
(30) Sheldrick, G. M. Acta Crystallogr. 2008, A64, 112−122. (31) Farrugia, L. J. J. Appl. Crystallogr. 2012, 45, 849−854.
(32) (a) Spek, A. L. J. Appl. Crystallogr. 2003, 36, 7−13. (b) Spek, A. L. Acta Crystallogr. 2009, D65, 148−155.
(33) Spalek, T.; Pietrzik, P.; Sojca, J. J. Chem. Ifn. Model. 2005, 45, 18−29.
(34) Case, D. A.; Darden, T. A.; Cheatham, T. E., III; Simmerling, C. L.; Wang, J.; Duke, R. E.; Luo, R.; Walker, R. C.; Zhang, W.; Merz, K. M.; Roberts, B.; Wang, B.; Hayik, S.; Roitberg, A.; Seabra, G.; I. ry, Wong, K. F.; Paesani, F.; Vanicek, J.; Liu, J.; Wu, X.; Brozell, S. R.; Steinbrecher, T.; Gohlke, H.; Cai, Q.; Ye, X.; Wang, J.; Hsieh, M.-J.; Cui, G.; Roe, D.R.; Mathews, D. H.; Seetin, M. G.; Sagui, C.; Babin, V.; Luchko, T.; Gusarov, S.; Kovalenko, A.; Kollman, P.A. AMBER 11, University of California, San Francisco, 2010.
(35) Wang, J.; Wolf, R. M.; Caldwell, J. W.; Kollman, P. A.; Case, D. A. J. Comput. Chem. 2004, 25, 1157−1174.
(36) Wang, J.; Wang, W.; Kollman, P. A.; Case, D. A. J. Mol. Graph.Model. 2006, 25, 247260.
(37) Darden, T.; York, D.; Pedersen, L. J. Chem. Phys. 1993, 98, 10089−10092.
(38) Ryckaert, J.-P.; Ciccotti, G.; Berendsen, H. J. C. J. Comput. Phys. 1977, 23, 327−341.
(39) Humphrey, W.; Dalke, A.; Schulten, K. J. Mol. Graph. 1996, 14, 33−38.

Table 1. Selected backbone torsional angles (in degrees) for compounds **5** and **7**·0.5C_6H_6.

	5		**7**·0.5C_6H_6	
C16-C17-N5-C19 (ϕ) N4-C16-C17-N5 (ψ)	-60.1(3) 136.3(2)	L-Ala	-57.2(3) 147.2(2)	L-Ala2
C11-C12-N4-C16 N3-C11-C12-N4 N2-N3-C11-C12	71.5(2) 69.4(2) 90.1(2)	D-Oxd	72.2(3) 64.8(3) 89.1(3)	D-Oxd2-Tri2
C27-C28-N10-C30 (ϕ) N9-C27-C28-N10 (ψ)			-70.1(4) 147.5(3)	L-Ala1-Tri1
C22-C23-N9-C27 N8-C22-C23-N9 N7-N8-C22-C23			70.7(4) 172.6(3) -101.0(3)	D-Oxd1-Tri1

Table 2 – K_D (mM) values for the Cu^{2+}-complexes with **6**, **8** and **10**. The λ values corresponding to the peak and through in the difference spectra as well as the Cu^{2+}-equivalents at system saturation are reported.

Compound	**λ*p* (nm)**	**λ*t* (nm)**	**K_D (mM)**	**Cu^{2+}-equivalents at saturation**
Boc-L-Ala-D-Oxd-Tri-COOH **6**	411	213	0.270	2
Boc-(L-Ala-D-Oxd-Tri-CO)$_2$-OH **8**	264	235	0.406	2-3
Boc-(L-Ala-D-Oxd-Tri-CO)$_3$-OH **10**	267	230	0.341	3

Table 3 – Hamiltonian parameters calculated from simulation of the EPR spectra of Cu^{2+}-complexes of compounds **6**, **8** and **10**, recorded at 77K.

Ligand	**Center**	**Contribution %**	$g_\perp$	$g_\parallel$	$A_\parallel$ (10^4 cm^{-1})	$A_\parallel$ (G)	$g_\parallel/A_\parallel$ (cm)
6	a	82	2.085	2.427	106.5	113.9	227.88
	b	18	2.069	2.364	125.7	134.4	188.06
8	a	70	2.085	2.425	109.1	116.7	222.27
	b	30	2.069	2.356	127.5	136.4	184.78
10	a	84	2.085	2.427	108.2	115.8	224.30
	b	16	2.070	2.362	133.3	142.6	177.19

.

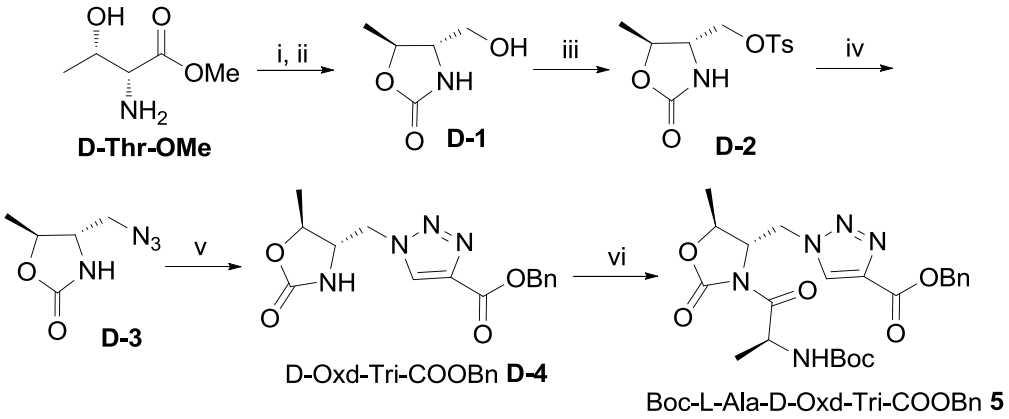

Scheme 1. Reagents and conditions: (i) trifosgene (1.1 equiv), THF, r.t., 1.h; (ii) $NaBH_4$ (1.1 equiv.), EtOH, r.t., 1.h, NH_4Cl, 45 min; (iii) TsCl (1.1 equiv.), DMAP (10% w/w), pyridine, r.t., 18 h; (iv) NaN_3 (1.1 equiv.), dry DMF, MW - 150 Watt/s, 25 min; (v) benzyl propiolate (1.0 equiv.), DIEA (2.0 equiv.), lutidine (2.0 equiv.), CuI (0.1 equiv.), dry acetonitrile, r.t., 2 h; (vi) Boc- Ala-OH (1.0 equiv.), HBTU (1.1 equiv.), Et_3N (2.0 equiv.), dry acetonitrile, r.t., 50 min.

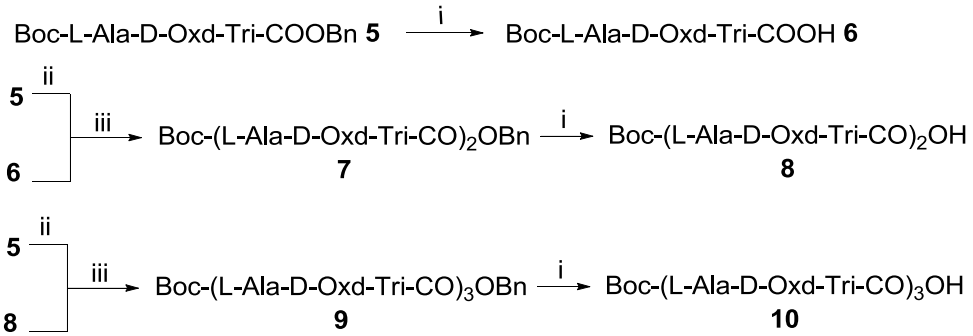

Scheme 2. Reagents and Conditions: (i) H_2, Pd/C (10%) (0.1 equiv.), MeOH, r.t., 16 h; (ii) TFA (18 equiv.), dry CH_2Cl_2, r.t., 4 h; (iii) HBTU (1.1 equiv.), Et_3N (2.0 equiv.), dry acetonitrile, r.t., 50 min.

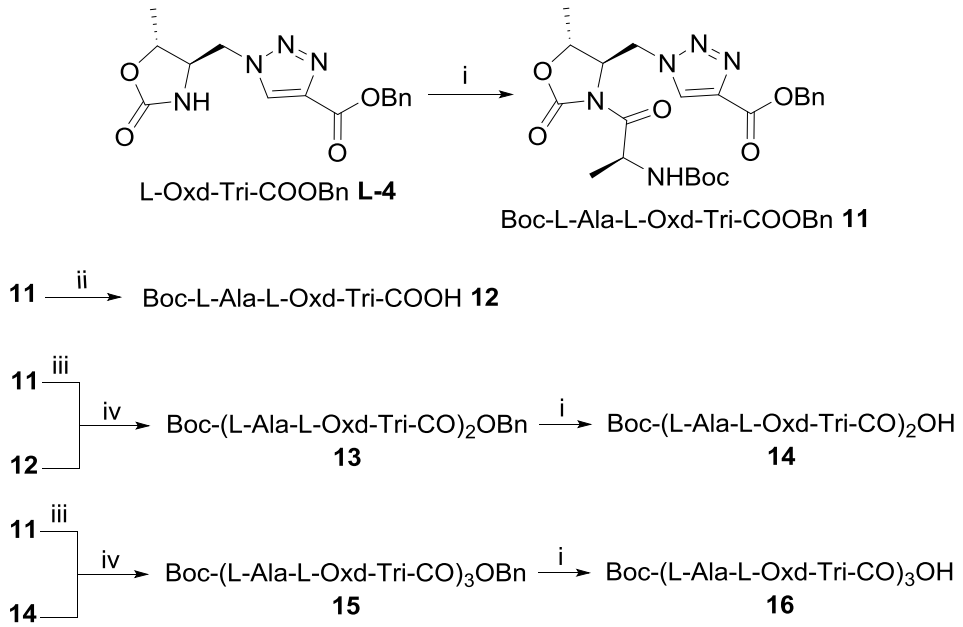

Scheme 3. Reagents and Conditions: (i) Boc-Ala-OH (1.0 equiv.), HBTU (1.1 equiv.), Et_3N (2.0 equiv.), dry acetonitrile, r.t., 50 min; (ii) H_2, Pd/C (10%) (0.1 equiv.), MeOH, r.t., 16 h; (ii) TFA (18 equiv.), dry CH_2Cl_2, r.t., 4 h; (iv) HBTU (1.1 equiv.), Et_3N (2.0 equiv.), dry acetonitrile, r.t., 50 min.

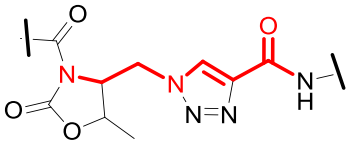

Figure 1. General structure of the Oxd-Tri scaffold. The preferential conformation of the imidic bond is shown. This scaffold is a constrained mimic of a ε-amino acid.

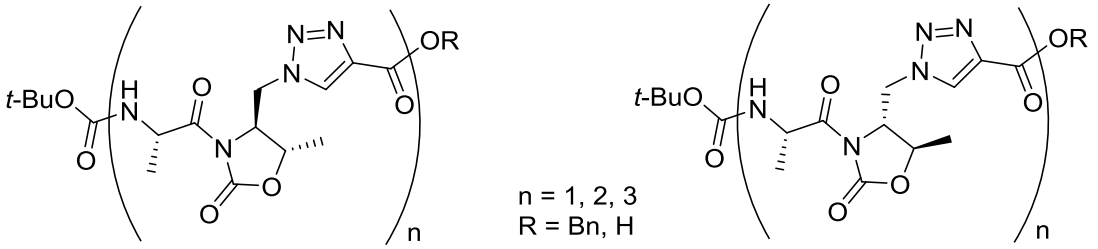

Figure 2. General formula of the oligomers investigated.

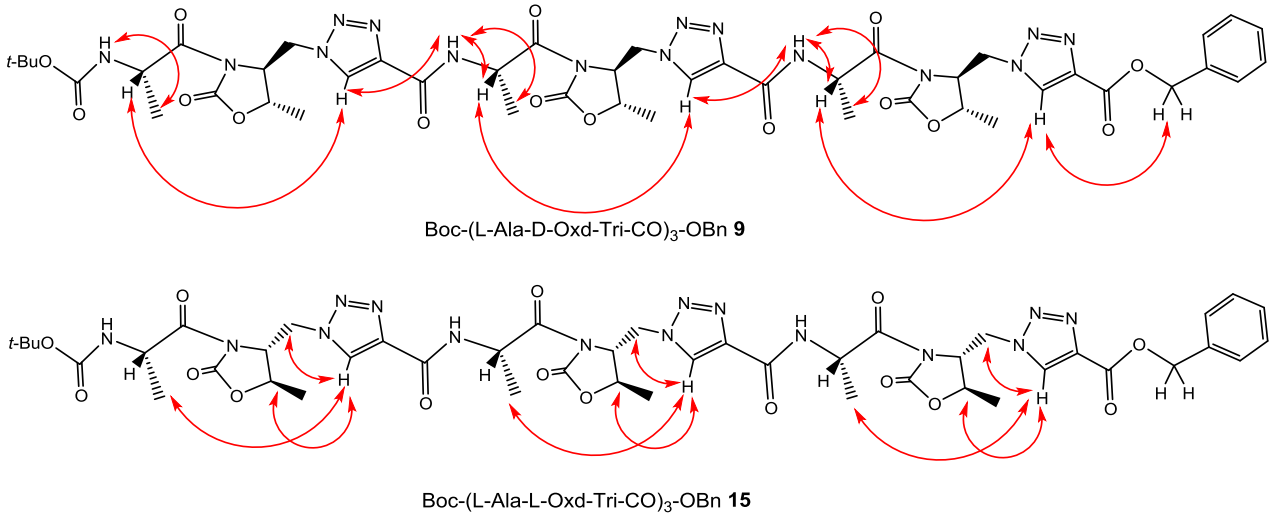

Figure 3. (top) NOE enhancements gathered from the ROESY spectrum analysis of **9** (top) and of **15** (bottom) (3 mM solution in $CDCl_3$, mixing time 0.400 s).

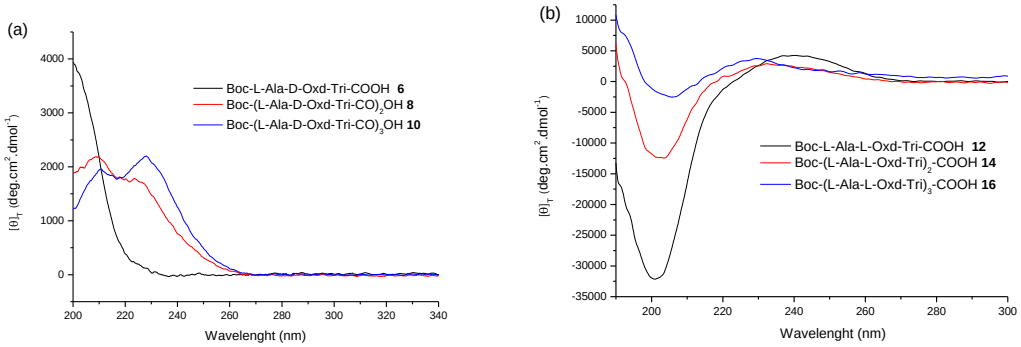

Figure 4. (a) Per-residue CD spectra of the oligomers of the L,D series: **6**, **8** and **10**; (b) per-residue CD spectra of the oligomers of the L,L series: **12**, **14** and **16**.

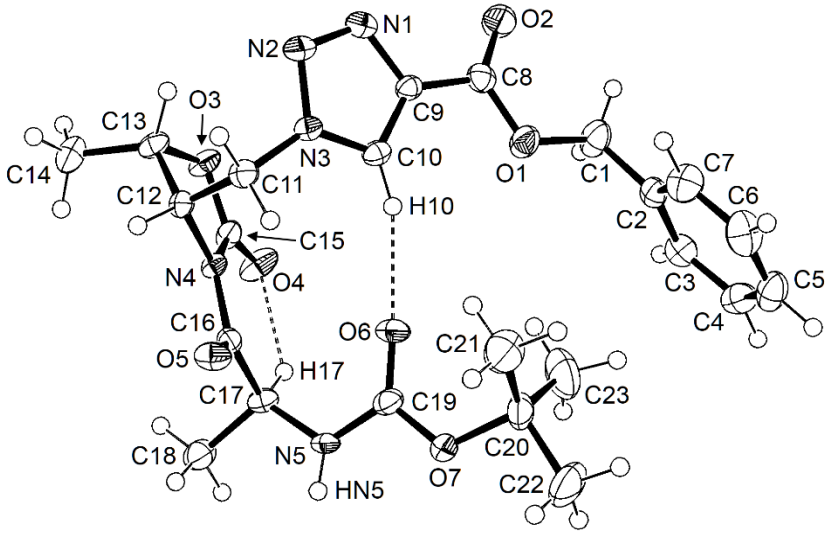

Figure 5 Ortep-3 [24] plot of **5** with thermal ellipsoids drawn at 50-% probability and H atoms represented as spheres of arbitrary radius. For simplicity, only H atoms engaged in intra- or intermolecular interactions are labelled. The dashed lines highlight intramolecular hydrogen bonding interactions discussed in the text.

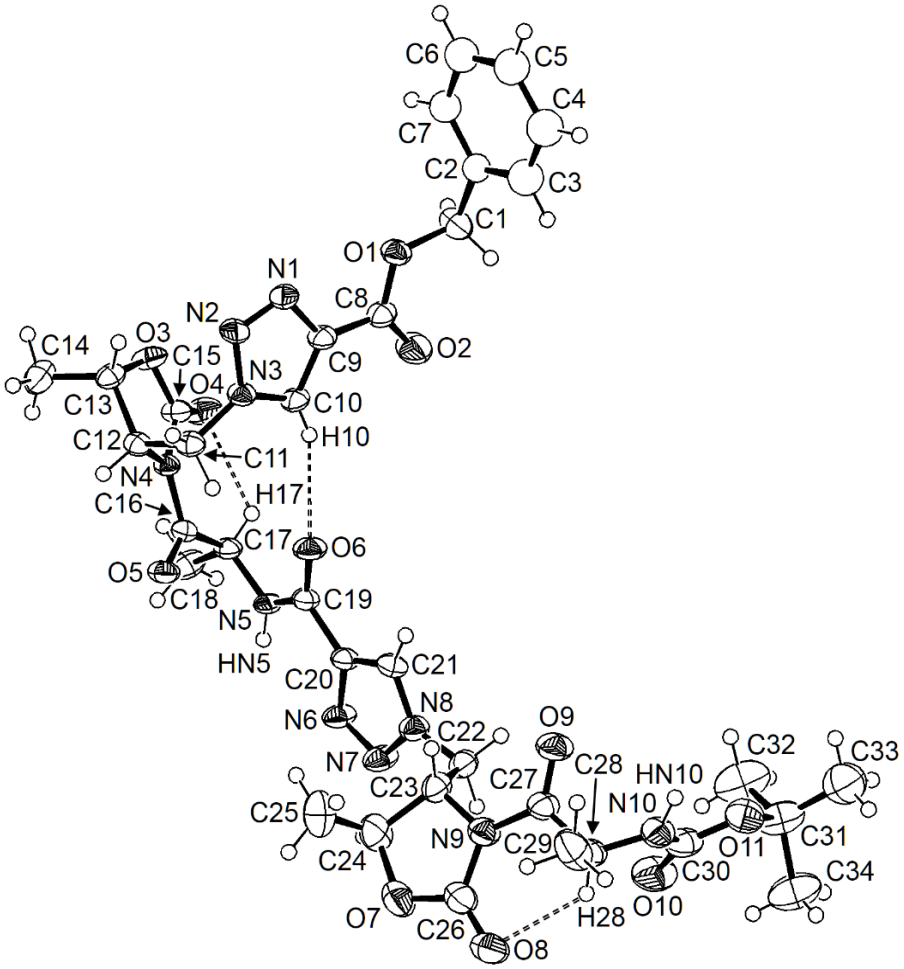

Figure 6. Ortep-3 [24] plot of **7** with thermal ellipsoids drawn at 50-% probability and H atoms represented as spheres of arbitrary radius. For simplicity, only H atoms engaged in intra- or intermolecular interactions are labelled. The dashed lines highlight intramolecular hydrogen bonding interactions discussed in the text.

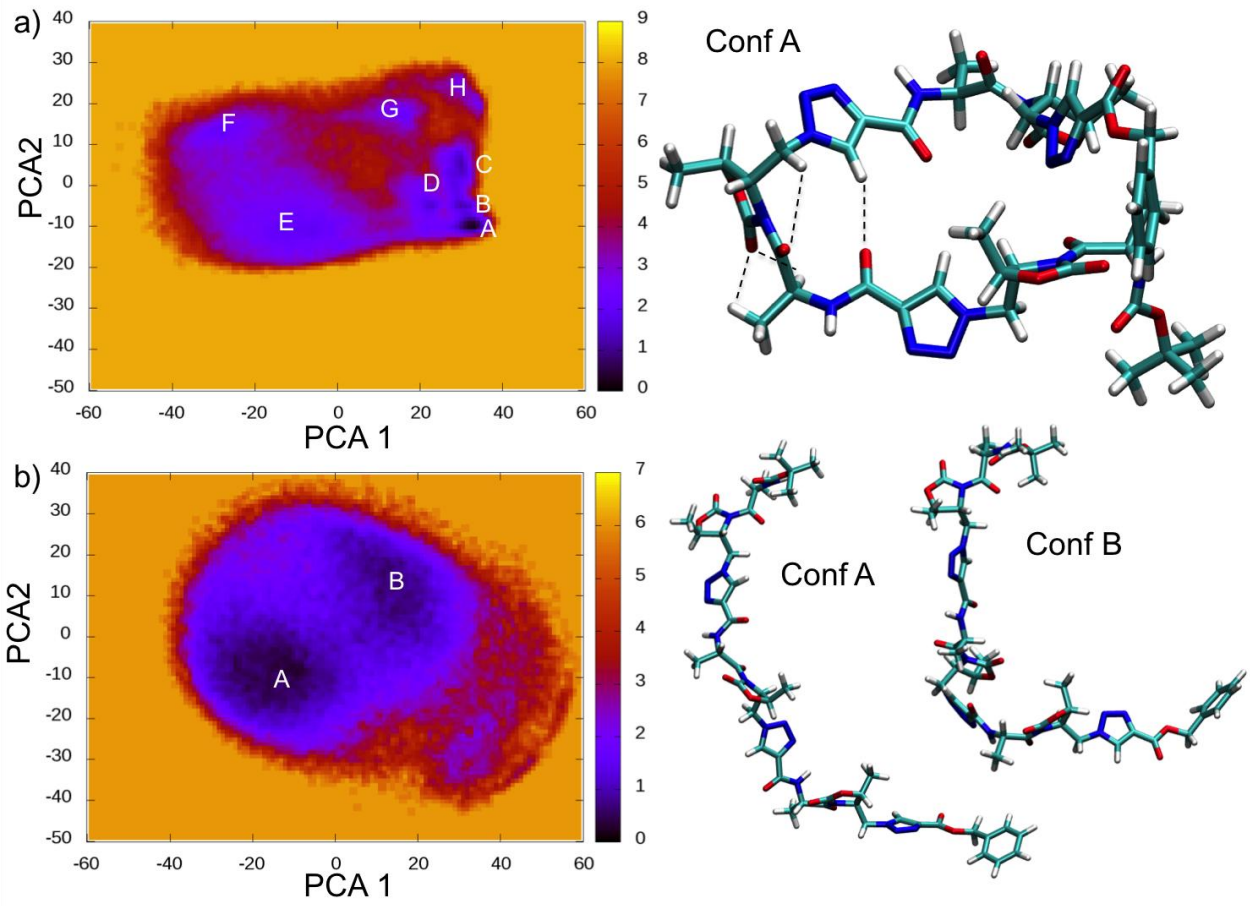

Figure 7. Conformational analysis of trimers **9** (a) and **15** (b). (Left) Two-dimensional free-energy landscape of the peptides, the values are in kcal mol^{-1}. The letters identify the most populated conformations. PCA1 and PCA2 are the two eigenvectors with the lowest eigenvalues of the principal component analysis calculated from the analysis of the MD trajectory. (Right) Representative structures of the conformational states corresponding to the most prominent minima of the free energy landscape.

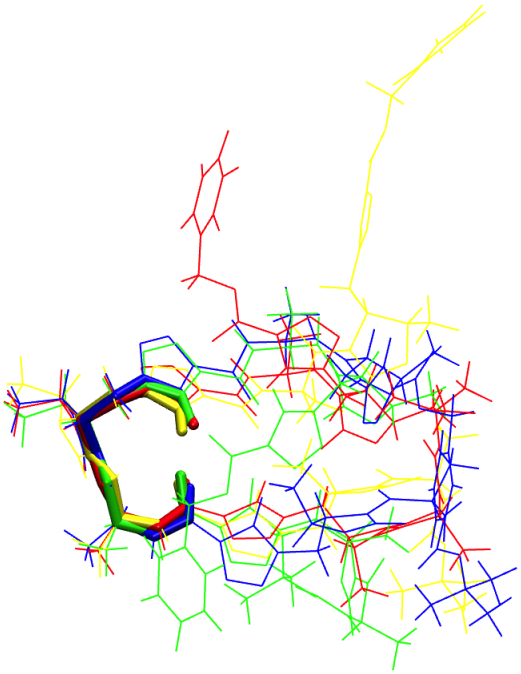

Figure 8. Superposition of the representative structures of the conformational states corresponding to Conf A (Blue), Conf B (Red); Conf C (Yellow) and Conf D (Green). In licorice the conserved structural motif of the eleven-membered hydrogen-bonded turn.

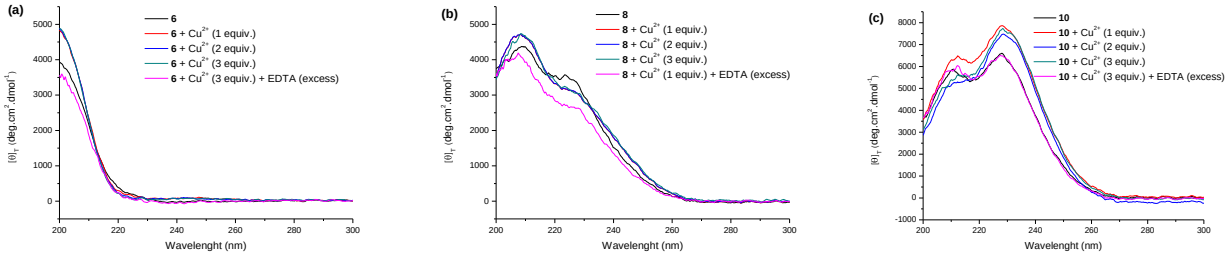

Figure 9. CD spectra of compounds **6**, **8** and **10** dissolved in MeOH/H_2O 8:2 v/v, in the absence and presence of Cu^{2+} and after addition of a molar excess of EDTA (a) **6** (0.419 mM); (b) **8** (0.246 mM) and (c) **10** (0.174 mM).